High-Resolution Methods for Hydrodynamics

William J. Rider

The decade of the 1980s saw a revolution in computational fluid dynamics that was driven by a new breed of algorithms known as high-resolution methods. The Advanced Simulation and Computing program of the Department of Energy provides the mechanism for making these methods available to weapons designers. When combined with advances in computing hardware, these methods will result in unprecedented computational fidelity within the weapons program.

Traditional Methods

We begin a discussion of traditional numerical hydrodynamics by considering the following prototypical equation:

$$\frac{\partial u}{\partial t} + \frac{\partial au}{\partial x} = 0 \, , \qquad (1)$$

where u is a function of t (time) and x (space), and a is a positive constant. This equation describes the advection, or transport, of the quantity u along the x-axis with velocity a. The flux associated with this advection process is the quantity au. The quantity u is con-served because the integral of u over the entire x-axis remains constant in time. As a result, Equation (1) is called a conservation equation. To solve Equation (1) numerically, we first defined a mesh consisting of discrete points in time and space. Let n denote the temporal index, and j denote the spatial index. The time step, Δt, is equal to $t^{n+1} - t^n$, and the spatial cell width, h, is equal to $x_{j+1} - x_j$ for all j. Once the mesh has been defined, a discretization scheme is used to evolve the function u in time. More specifically, given all values of u on the spatial mesh at time n, a discretization scheme is used to compute all values of u on the mesh at time $n + 1$. We first consider two tra-
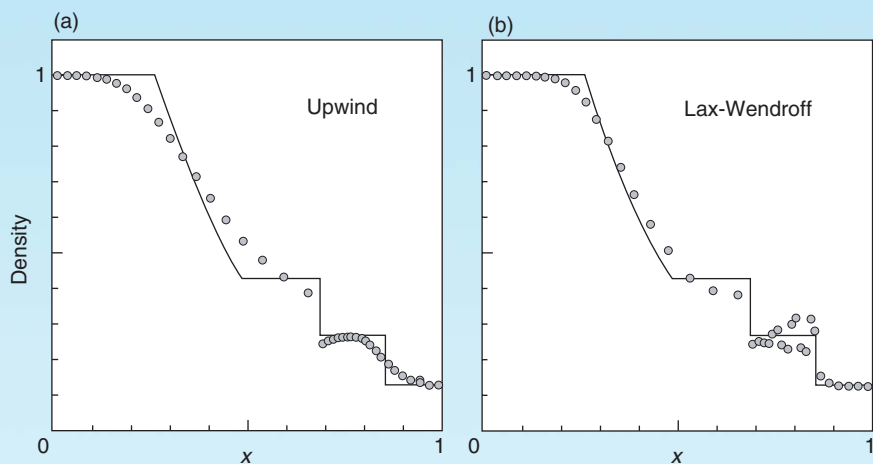

(a)   Upwind

(b)   Lax-Wendroff

Figure 1. Simulated and Exact Density Profiles for a Shock Tube Problem
The shock tube problem begins with a membrane between two quiescent gases at different pressures and densities. When the membrane is broken, a complex wave interaction is initiated. The solution shown here corresponds to the material density as a function of position at a specific time after the membrane has been broken. The exact solution (solid line) results from solving this so-called Riemann problem. In (a) and (b), the analytic solution is compared with the solutions calculated with the simple first-order upwind method and the second-order Lax-Wendroff method, respectively. The plots in (a) and (b) illustrate the basic tradeoff between monotonic-dissipative and oscillatory-dispersive discretization techniques.

ditional discretization schemes for solving Equation (1). The first is the simple upwind scheme,

$$u_j^{n+1} = u_j^n - \lambda\left(u_j^n - u_{j-1}^n\right) , \qquad (2)$$

where $\lambda = a\Delta t/h$, and the second is the Lax-Wendroff scheme,

$$u_j^{n+1} = u_j^n - \lambda\left(u_{j+1}^n - u_{j-1}^n\right)\!\Big/2$$
$$+ \lambda^2\left(u_{j+1}^n - 2u_j^n + u_{j-1}^n\right)\!\Big/2 . \qquad (3)$$

Assuming that the solution for u is smooth, we can use a form of Taylor series analysis to determine the associated error with the discretization scheme. For instance, the error associated with the simple upwind scheme is

$$E_{UP} = h\frac{|a|}{2}\frac{\partial^2 u}{\partial x^2} + O\!\left(h^2\right) , \qquad (4)$$

where $O(h^2)$ denotes terms proportional to h^k, where k is an integer greater than or equal to 2. The upwind scheme is said to be first-order accurate because its error is proportional to h. The error associated with the Lax-Wendroff scheme is

$$E_{LW} = h^2\frac{a}{6}\frac{\partial^3 u}{\partial x^3} + O\!\left(h^3\right) . \qquad (5)$$

The Lax-Wendroff scheme is second-order accurate. If the cell width is decreased by a factor of 2, the error associated with a first-order scheme decreases by a factor of 2 (2^1), but the error associated with a second-order method decreases by a factor of 4 (2^2). Traditional second-order methods tend to be significantly more accurate than first-order methods, but they tend to oscillate badly when solutions are not smooth, that is, when discontinuities are present. Furthermore, they can be dispersive in that a single wave can nonphysically break up into several smaller waves. The problem with oscillations is that they can produce unphys-

ical states in the calculation, such as negative densities or pressures. First-order methods do not oscillate when shocks are present, but they tend to significantly broaden shock fronts and dissipate energy. These properties are illustrated in Figure 1, where a shock tube problem is solved with the first-order upwind and the second-order Lax-Wendroff methods. Because solutions with shocks are not smooth, the Taylor series analysis used to characterize the accuracy of the upwind and Lax-Wendroff schemes is not valid. In fact, all discretization schemes are first-order accurate for problems with shocks. Nonetheless, as is clear from Figure 1, the errors exhibited by different schemes for such problems can be far different in magnitude and character.

High-Resolution Methods

An essential element of high-resolution discretization schemes is nonlinearity. This property follows in part from a very important theorem, originally developed by Sergei Godunov, which states that a second-order linear discretization cannot produce monotone (nonoscillatory) solutions to Equation (1). Godunov's theorem motivated researchers to investigate the addition of nonlinearities to discretization schemes, and this study resulted in a major breakthrough. High-resolution discretization schemes are generally constructed from three linear schemes: one is first order and monotone, and two are second order. These schemes are then combined in a manner that ensures second-order accuracy when the solution is smooth and both high
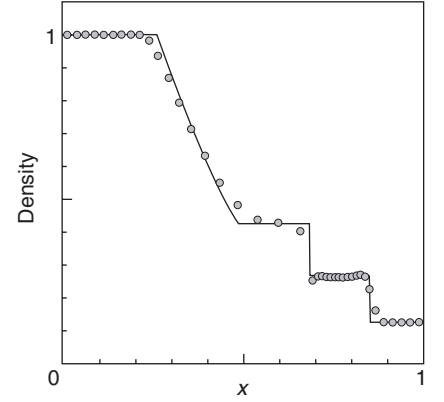

Figure 2. High-Resolution Solution to the Shock Tube Problem
The high-resolution method results in a solution to the shock tube problem that very closely matches the analytic solution (solid line).

accuracy and monotonicity when the solution is not smooth. At the heart of this approach is a nonlinear limiter that effectively switches between definitions for certain terms, depending upon the local behavior of the solution. For instance, an example of a simple high-resolution method is provided in the box below—compare with Equations (2) and (3):

$$u_j^{n+1} = u_j^n - \lambda\left(u_j^n - u_{j-1}^n\right)$$
$$- \lambda(1-\lambda)\left(\phi_j^n - \phi_{j-1}^n\right)\!\Big/2 , \qquad (6)$$

where the limiter, ϕ, is defined as follows:

$$\phi_j^n = \left(u_j^n - u_{j-1}^n\right)\max\left[0,\min\left(1,\left(\left(u_{j+1}^n - u_j^n\right)\!\Big/\!\left(u_j^n - u_{j-1}^n\right)\right)\right)\right] . \qquad (7)$$

This method was used to obtain the numerical solution plotted in Figure 2. The high-resolution solution shows a dramatic increase in accuracy over the two solutions plotted in Figure 1. A very important property of high-resolution methods relates to their unique ability to model turbulent behavior. Traditional methods are
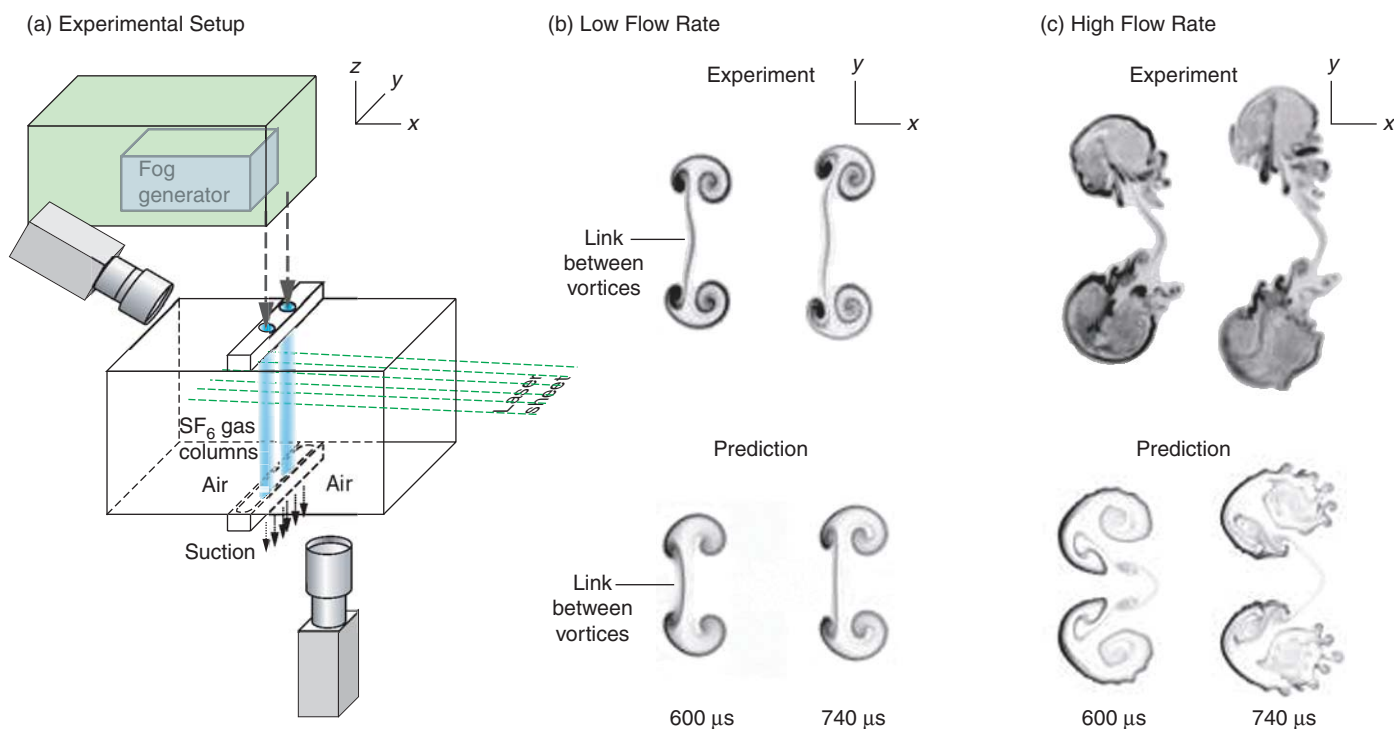
(a) Experimental Setup

(b) Low Flow Rate

(c) High Flow Rate

Figure 3. Simulating Richtmyer-Meshkov Experiments at Low and High Flow Rates
Panel (a) shows an experiment to study the Richtmyer-Meshkov instability in which two columns of SF_6 gas (with density five times that of air) flow downward through the test section under the force of gravity and are hit by a planar shock wave with Mach number 1.2. The shock deposits vorticity along the cylinder edges, which distorts them into a "mushroom cap" shape. Images of the unstable structures are captured by laser-sheet visualization at two times after the passage of the shock. Panels (b) and (c) compare experimental and simulated results for experiments at low flow rate (and Reynolds number) and high flow rate (and Reynolds number), respectively. The simulations used the xPPM method implemented in the computer code Cuervo. Both simulations successfully model the gross features of the flow, including links between the two gas columns. (This work was conducted jointly with Christopher Tomkins, Robert Benjamin, and James Kamm of Los Alamos).

essentially unable to model such behavior. The latest high-resolution, known as second-generation, methods appear to be particularly useful for computing turbulent flows. The ultimate litmus test for computational methods and modeling is a direct comparison with experiment. A shock wave can induce turbulent mixing between two materials. This phenomenon is known as the Richtmyer-Meshkov instability, and it is important in situations arising in astrophysics, high explosives, and inertially confined fusion experiments. For the past 5 years, we have been working very closely with experimentalists to validate our methods for modeling the development of instabilities. Using one of our new second-generation methods, xPPM,

we computed the mixing of two cylinders of sulfur hexafloride gas with a background gas (air). The simulation showed a bridge of material linking the two cylinders late in the experimental time. Although the link was heretofore unobserved, when the experimentalists succeeded in improving their ability to monitor the evolution of the instability, they discovered that the link was indeed present at both low and high flow rates (see Figure 3). The graphic on the opening page is a later result comparing first- and second-generation high-resolution results for a single gas column (calculated with Jeff Greenough of Lawrence Livermore National Laboratory). In the future, we hope to make more quantitative comparisons between experiments

and turbulent flows calculated with our second-generation methods. Finding ways to achieve this goal is a research topic in itself. ∎

For further information, contact Bill Rider (505) 665-4162 (rider@lanl.gov).